

Synthesis and thermal decomposition studies of homo- and heteroleptic tin(IV) thiolates and dithiocarbamates: molecular precursors for tin sulfides

Giampaolo Barone,^{†a} Tracy Chaplin,^b Thomas G. Hibbert,^a Aliko T. Kana,^a Mary F. Mahon,^a Kieran C. Molloy,^{*a} Ian D. Worsley,^a Ivan P. Parkin^b and Louise S. Price^b

^a Department of Chemistry, University of Bath, Claverton Down, Bath, UK BA2 7AY

^b Department of Chemistry, University College London, 20 Gordon Street, London, UK WC1H 0AJ

Received 19th September 2001, Accepted 14th November 2001

First published as an Advance Article on the web 18th February 2002

The syntheses and X-ray structures of novel heteroleptic thiolate/dithiocarbamate derivatives $(Et_2NCS_2)_2(RS)_2Sn$ ($R = Cy, CH_2CF_3$) have been examined and their thermal decompositions compared with those of selected tin(II) and tin(IV) dithiocarbamates. The heteroleptic species decompose to SnS by initial elimination of RSSR to afford $(Et_2NCS_2)_2Sn$ and subsequent loss of $[Et_2NC(S)]_2S$. In contrast, $(Et_2NCS_2)_4Sn$ decomposes via $[(Et_2NCS_2)_2SnS]_2$, whose structure has been determined, and finally to SnS₂ by sequential elimination of $[Et_2NC(S)]_2S$. The two families of compounds, $(R_2NCS_2)_4Sn$ and $(Et_2NCS_2)_2(RS)_2Sn$, thus provide single-source materials for bulk SnS₂ and SnS, respectively, by virtue of their differing decomposition pathways. Preliminary CVD experiments with $(Et_2NCS_2)_2(CyS)_2Sn$ are also reported.

The study of tin(IV) oxide films is a well established field, fuelled by the commercial exploitation of these materials as optically transparent, wide bandgap semiconductors. Related tin sulfide materials, though less studied, are the focus of much recent interest.¹ SnS has an optical bandgap of 1.3 eV and its films have potential applications as photovoltaic materials, holographic recording systems^{2,3} and solar control devices.⁴ SnS₂, a wider bandgap n-type semiconductor, has been much less intensely studied, but it is known that its layered structure (in contrast to the rutile structure of SnO₂) permits intercalation of alkali metals⁵ and metallocenes^{6,7} with resulting increases in conductivity. The deposition of tin sulfide is, however, a potentially complex problem as a range of possible materials could plausibly result. SnS (herzenbergite), a variety of non-stoichiometric Sn_{1+x}S phases, SnS₂ (berndtite), for which 70 polytype structures have been identified), Sn₂S₃ (ottemannite, three polytypes) and Sn₄S₅ have all been cited in a recent review of this area.¹

Tin sulfide films have been prepared by spray pyrolysis,⁸ melt growth,⁹ electrodeless deposition¹⁰ and chemical baths,^{11,12} while bulk SnS has been prepared *inter alia* by thermal decomposition of the molecular precursors $(Ph_3Sn)_2S$ (>300 °C)¹³ and $(Bz_2SnS)_3$ (450 °C).¹⁴ However, in contrast to the preparation of tin oxide films where chemical vapour deposition (CVD) from an appropriate precursor or precursors is common, this methodology has been largely ignored for tin sulfide films. SnS has been speculated as the product deposited on either CaF₂ or MgF₂ from R₄Sn/H₂S/H₂ mixtures ($R = Me, Et$),¹⁵ while CVD using SnCl₄/H₂S/H₂ has been shown to generate chlorine-contaminated SnS_{0.75}.¹⁶ We have recently reported the deposition of tin sulfides from a dual-source approach using H₂S and either SnCl₄,^{17,18} SnBr₄¹⁹ or Bu₃SnO₂CCF₃.²⁰ We have also found that potential single-source precursors such as $(PhS)_4Sn$ ²¹ also require the use of H₂S as co-reagent, though

chelating dithiolates *e.g.* Sn(SCH₂CH₂S)₂ obviate the need for a co-reagent.²²

We now report the preparation and properties of a number of further CVD candidates for evaluation. Dithiocarbamate derivatives of tin were considered the most promising species, as analogous compounds have been used effectively in other areas of metal chalcogenide deposition.²³ For example, ZnS and CdS have been deposited from $M[S_2CN(Me)CH_2CH_2CH_2NMe_2]_2$ ($M = Zn, Cd$) at low pressures.²⁴ Tin(IV)^{25,26} and tin(II)^{27,28} dithiocarbamate derivatives have been known since the 1970s. In addition to homoleptic tin dithiocarbamates, we have also considered heteroleptic species containing both dithiocarbamate and thiolate ligands *i.e.* $(R_2NCS_2)_n(RS)_{4-n}Sn$ as possible precursors, as well as being interesting synthetic and structural targets in their own right. From the CVD perspective, the use of hybrid alkoxide/β-diketonates is widespread²⁹ but an analogous strategy for heavier Group 16-containing materials has not, to our knowledge, been considered previously.

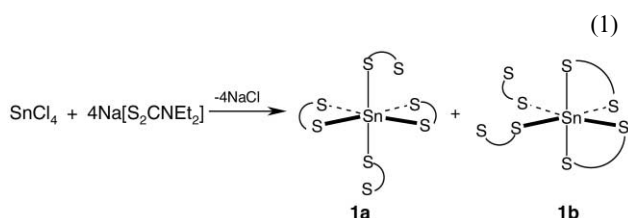
Results and discussion

Synthetic and structural chemistry

$(Et_2NCS_2)_4Sn$ (**1**), was synthesised by a literature route from SnCl₄ and $[Et_2NCS_2]Na$.²⁵ The structure of this compound is known²⁵ showing that two of the dithiocarbamate ligands are bidentate, the other two being monodentate, and these latter ligands are arranged in a *trans*-orientation about tin (**1a**). Interestingly, the ¹¹⁹Sn NMR spectrum of an analytically pure sample of **1** showed three, closely spaced resonances at -766 (100%), -764 (30%) and -768 ppm (32%), which are not sidebands but which we speculatively assign to the presence of both *trans*-(**1a**) and *cis*-(**1b**) isomers of **1** in solution. We assign the major resonance to **1a** as this is the one that has been isolated by others and whose structure has been determined.²⁶ One of the remaining species is likely to be **1b**, while the third we speculate is an isomer of either **1a,b** in which the orientation of the dative and covalent Sn-S bonds in the two chelating dithio-

[†] On leave from: Dipartimento di Chimica Inorganica, Università di Palermo, Via Arcirafi 26-28, Palermo 90123, Italy.

carbamate groups differ. For comparison, we have synthesised the novel unsymmetrical tin dithiocarbamate $[\text{Bu}^n(\text{Me})\text{NCS}_2]_4\text{-Sn}$ (**2**) but this shows a single major resonance at -786 ppm along with an unidentified minor impurity at -724 ppm (12%).



On standing, a solution of **1** in either CHCl_3 or CH_2Cl_2 starts to decompose even at room temperature as evidenced by a colour change from orange to pale yellow, a process which can be accelerated by heating. Pale yellow crystals can be isolated and have been identified as the dimeric sulfide $[(\text{Et}_2\text{NCS}_2)_2\text{SnS}]_2$ (**3**). The formation of **3** is of interest as it is an intermediate in the thermal decomposition of **1** to SnS_2 (see below). After 24 h at room temperature, the ^{119}Sn NMR of **1** in CDCl_3 shows a new resonance at -736 ppm, which is identical to that shown by a solution of crystals of **3**. A second species with $\delta(^{119}\text{Sn})$ of -705 ppm also appears, and, although this is as yet unidentified, it is not *cis*- $(\text{Et}_2\text{NCS}_2)_2\text{SnCl}_2$ [$\delta(^{119}\text{Sn}) -519$ ppm].³⁰

The structure of **3** is shown in Fig. 1. The sulfide bridges

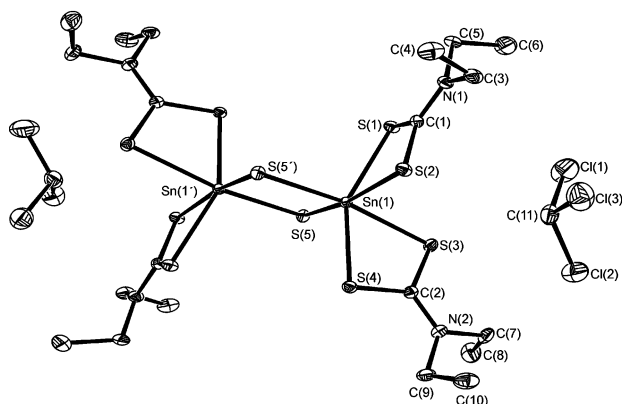


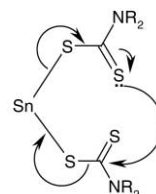
Fig. 1 The molecular unit of **3**; thermal ellipsoids are at the 30% probability. Primed atoms are related to their unprimed counterparts in the asymmetric unit by $-x, -y, 1-z$. Sn(1)–S(1) 2.5676(5), Sn(1)–S(2) 2.5986(5), Sn(1)–S(3) 2.6075(5), Sn(1)–S(4) 2.5772(5), Sn(1)–S(5) 2.4454(5), Sn(1)–S(5') 2.4550(5) Å; S(1)–Sn(1)–S(2) 69.84(2), S(1)–Sn(1)–S(3) 89.30(2), S(1)–Sn(1)–S(4) 150.03(2), S(1)–Sn(1)–S(5) 98.96(2), S(1)–Sn(1)–S(5') 100.74(2), S(2)–Sn(1)–S(3) 88.74(2), S(2)–Sn(1)–S(4) 88.21(2), S(2)–Sn(1)–S(5) 168.75(2), S(2)–Sn(1)–S(5') 89.60(2), S(3)–Sn(1)–S(4) 69.44(1), S(3)–Sn(1)–S(5) 92.31(1), S(3)–Sn(1)–S(5') 168.56(2), S(4)–Sn(1)–S(5) 102.65(2), S(4)–Sn(1)–S(5') 99.19(2), S(5)–Sn(1)–S(5') 91.53(2).

enforce a *cis, cis, cis* geometry on the ligands and the Sn–S(sulfide) bonds [2.4454(5), 2.4550(5) Å] are typical of other dimeric organotin sulfides containing six-coordinated tin *e.g.* $\{[\text{CyNC}(\text{Me})\text{NCy}]_2\text{Sn}\}_2\text{S}$: 2.434, 2.476 Å,³¹ but longer than in analogous dimers in which tin is only four-coordinated *e.g.* $(\text{Bu}^n_2\text{SnS})_2$: 2.419, 2.441 Å.³² The two dithiocarbamate groups chelate in an anisobidentate manner [2.5676(5), 2.5986(5); 2.5772(5), 2.6075(5) Å for each pair of ligands, respectively], similar to that of **4** (below). The longer Sn–S bond in each dithiocarbamate is *trans* a bridging sulfur centre.

The mechanism of formation of **3** at room temperature from solutions of **1** in chlorinated solvents is of importance. Interestingly, the appearance of a signal due to **3** in the NMR of **1** is accompanied by a decrease in the intensity of the minor signal at -768 ppm, which we have tentatively assigned to **1b**. We speculate that the *cis*-arrangement of dithiocarbamate groups in **3** requires a similar stereochemistry in **1** for the elimination

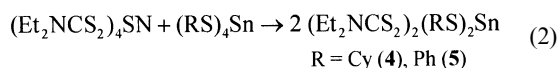
of $(\text{Et}_2\text{NCS}_2)_2\text{S}$ to take place. Thus, the conversion of the major isomer **1a** to **3** uses the minor isomer **1b** as intermediate.

While older TGA studies on the thermal decomposition of $(\text{Et}_2\text{NCS}_2)_4\text{Sn}$ have claimed elimination of $(\text{Et}_2\text{NCS}_2)_2$ followed by sulfur extrusion [to afford $(\text{Et}_2\text{NCS}_2)_2\text{S}$] and subsequent oxidative addition to $(\text{Et}_2\text{NCS}_2)_2\text{Sn}$ as the route by which species such as **3** are formed,³³ the fact that decomposition can take place at room temperature suggests this is unlikely, at least in chlorinated solvents. Again, we speculate that a *cis*-arrangement of monodentate dithiocarbamate groups allows the formation of **3** by a concerted mechanism (chelating groups omitted for clarity):

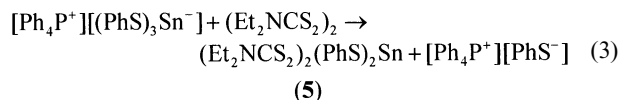


$(\text{R}_2\text{NCS}_2)_4\text{Sn}$ (R = 4-methylpiperidine) has previously been reported to decompose in chlorinated solvents, but is reported as yielding the dimeric disulfide $[(\text{R}_2\text{NCS}_2)_2\text{SnS}]_2$ only on prolonged reflux in CH_2Cl_2 .³⁴

In order to increase the variety of compounds available for CVD trials, we have prepared the first examples of mixed thiolate/dithiocarbamate derivatives of tin(IV). Compound **1** was stirred at room temperature with $(\text{CyS})_4\text{Sn}$ in toluene, giving $(\text{Et}_2\text{NCS}_2)_2(\text{C}_6\text{H}_{11}\text{S})_2\text{Sn}$ (**4**) as bright yellow crystals. Interestingly, **4** was the only product from these reactions regardless of the relative stoichiometries of the reactants.



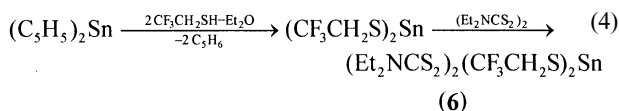
$(\text{Et}_2\text{NCS}_2)_2(\text{PhS})_2\text{Sn}$ (**5**) can, however, be prepared similarly or from the reaction of $[\text{Ph}_4\text{P}^+][(\text{PhS})_3\text{Sn}^-]$ with tetraethylthiuram disulfide (eqn. 3). We have no evidence for the form-



ation of the anticipated product $[\text{Ph}_4\text{P}^+][(\text{PhS})_3(\text{Et}_2\text{NCS}_2)_2\text{Sn}^-]$ though it is plausible that this is an intermediate in the formation of **5**.

Compound **5** has also been obtained from the reaction of **1** with $(\text{Et}_2\text{NCS}_2)_2\text{Cu}$.

We have also been able to prepare the fluoroalkylthiolatotin species $(\text{Et}_2\text{NCS}_2)_2(\text{CF}_3\text{CH}_2\text{S})_2\text{Sn}$ (**6**) by oxidative addition of tetraethylthiuram disulfide to $(\text{CF}_3\text{CH}_2)_2\text{Sn}$, prepared *in situ* from $(\text{C}_5\text{H}_5)_2\text{Sn}$ and two equivalents of $\text{CF}_3\text{CH}_2\text{SH}$.



Compounds **4–6** are characterised by large upfield shifts in their ^{119}Sn NMR resonances (-649 to -666 ppm), in contrast to the downfield shifts of the four-coordinate species $(\text{RS})_4\text{Sn}$ *e.g.* $(\text{CyS})_4\text{Sn}$, $\delta(^{119}\text{Sn})$: 109 ppm.³⁵

Surprisingly, the unsymmetrical tetrakis(dithiocarbamato)-tin(IV) species $[\text{Bu}^n(\text{Me})\text{NCS}_2]_4\text{Sn}$ (**2**) fails to react with $(\text{RS})_4\text{Sn}$ nor does it undergo decomposition in chlorinated solvents to form a sulfide-bridged dimer analogous to **3**. The *cis*-stereochemistry of dithiocarbamates in each of **3, 4–6** suggests that the absence of any *cis*-isomer of **2** is responsible.

Reports of mixed thiolate/dithiocarbamate metal complexes are rare and we are aware of only six citations in the Cambridge Crystallographic Database: 36 $\text{Mo}_2\text{O}_2(\text{S})(\text{SCH}_2\text{CH}_2\text{O})(\text{S}_2\text{CNET}_2)_2$, 37 $\text{Co}_2(\text{SEt})_2(\text{S}_2\text{CSEt})(\text{S}_2\text{CNET}_2)_3$, 38 $\text{NCr}(\text{NPr})[(\text{SBu}^+)\text{Cu}(\text{S}_2\text{CNET}_2)_2]$, 39 $\{(\text{MeS})[\text{Me}(\text{H})\text{NCS}_2]\text{Ni}\}_2$, 40 $(\text{Et}_3\text{P})(\text{Me}_2\text{NCS}_2)(\text{SMe})\text{Pd}$, 41 $[\text{Rh}(\text{S}_2\text{CNET}_2)_2]_2(\text{SCH}_2\text{CH}_2\text{SCH}_2\text{CH}_2\text{SCH}=\text{CH}_2)_2$. 42 This type of compound offers a general route to tailoring both the volatility and decomposition pathway of the precursors and it is surprising that species of this type have remained unexplored. In contrast, mixed alkoxide/ β -diketonates, which are the analogous monodentate/bidentate hybrid oxygenated precursors for the deposition of metal oxides, have been widely exploited. 29

The crystal structure of **4** is shown in Fig. 2, along with

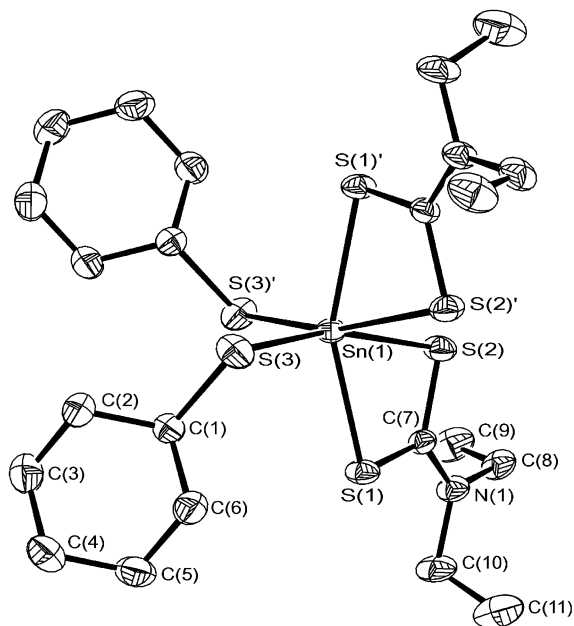


Fig. 2 The molecular unit of **4**; thermal ellipsoids are at the 30% probability. Primed atoms are related to their unprimed counterparts in the asymmetric unit by $1 - x, y, 1/2 - z$; thermal ellipsoids are at the 30% probability. Selected metric data: Sn(1)–S(3) 2.450(1), Sn(1)–S(1) 2.570(1), Sn(1)–S(2) 2.618(1) Å; S(3')–Sn(1)–S(3) 100.68(8), S(3')–Sn(1)–S(1) 98.88(5), S(3)–Sn(1)–S(1) 95.29(5), S(1')–Sn(1)–S(1) 157.72(7), S(3)–Sn(1)–S(2') 87.49(5), S(1)–Sn(1)–S(2') 94.60(4), S(3)–Sn(1)–S(2) 163.46(4), S(1)–Sn(1)–S(2) 69.07(4), S(2')–Sn(1)–S(2) 88.44(7)°.

selected bond lengths and angles. It can be seen that the dithiocarbamate ligands adopt a *cis*-conformation in contrast to the *trans*-conformation found for **1**, while the two thiolate groups are also mutually *cis*. In addition, the ^{119}Sn NMR spectrum of **3** shows only one resonance (-649 ppm) suggesting that there is no mixture of *cis*- and *trans*-isomers present in solution. The *cis*-(RS) $_2$ (S $_2$ CNR $_2$) $_2$ Sn arrangement is in contrast to the known diorganotin bis(dithiocarbamate) structures [e.g. $\text{Me}_2\text{Sn}(\text{S}_2\text{CNR}_2)_2$, R = Me, 43 Et 44] which have *trans*-R $_2$ Sn(S $_2$ CNR $_2$) $_2$ stereochemistry about the tin. $\text{Bu}^t_2\text{Sn}(\text{S}_2\text{CNMe}_2)_2$ 45 does possess the alkyl groups in a *cis*-conformation, but in this case only one of the dithiocarbamate ligands is bidentate. The Sn–S(thiolate) bond lengths in **4** are identical [2.450(1) Å] but somewhat longer than those in four-coordinated (CyS) $_4$ Sn [2.382(1) Å]. 35 The two dithiocarbamate ligands are also equivalent, both being slightly anisobidentate [Sn–S(1) 2.570(1); Sn–S(2) 2.618(1) Å]. In all the comparable diorganotin bis(dithiocarbamate) structures the bidentate dithiocarbamates are also anisobidentate, with the divergence from isobidentate behaviour more marked than in **4**.

Compound **6** (Fig. 3) adopts the same stereochemistry as **4** with *cis*-thiolate and *cis*-dithiocarbamate groups. The effect of the electron withdrawing CF_3 groups seems to be enhancement

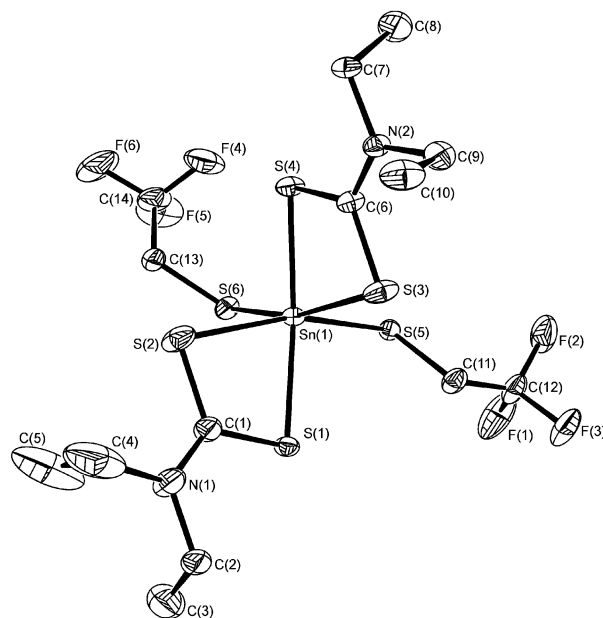


Fig. 3 The asymmetric unit of **6**; thermal ellipsoids are at the 30% probability. Selected metric data: Sn(1)–S(1) 2.5535(7), Sn(1)–S(2) 2.5650(9), Sn(1)–S(3) 2.5774(9), Sn(1)–S(4) 2.5625(8), Sn(1)–S(5) 2.4745(8), Sn(1)–S(6) 2.4575(8) Å; S(6)–Sn(1)–S(5) 84.10(3), S(6)–Sn(1)–S(1) 103.98(3), S(5)–Sn(1)–S(1) 94.42(2), S(6)–Sn(1)–S(4) 95.87(3), S(5)–Sn(1)–S(4) 105.58(3), S(1)–Sn(1)–S(4) 153.15(3), S(6)–Sn(1)–S(2) 94.53(4), S(5)–Sn(1)–S(2) 164.17(3), S(1)–Sn(1)–S(2) 70.55(3), S(4)–Sn(1)–S(2) 90.25(3), S(6)–Sn(1)–S(3) 165.38(3), S(5)–Sn(1)–S(3) 94.12(3), S(1)–Sn(1)–S(3) 90.62(3), S(4)–Sn(1)–S(3) 70.57(3), S(2)–Sn(1)–S(3) 91.06(4)°.

of the Lewis acidity of tin, resulting in stronger Sn–S(dtc) bonds [Sn(1)–S(1) 2.5535(7), Sn(1)–S(4) 2.5625(8) Å] and more symmetrical chelation [Sn(1)–S(2) 2.5650(9), Sn(1)–S(3) 2.5774(9) Å] by the dithiocarbamate ligands; the Sn–S(thiolate) bonds weakened as a result [Sn(1)–S(5) 2.4745(8), Sn(1)–S(6) 2.4575(8) Å]. The other noteworthy difference between **4** and **6** is the \angle S–Sn–S involving the two thiolate ligands. This angle is much smaller for **6** [84.10(3)°] than **4** [100.68(8)°]. We believe the explanation for this to lie in the conformations of the C–S–Sn–S units which for **6** adopt an arrangement approaching *trans*-, *trans*-(*ap*, *ap*); dihedral \angle C–S–Sn–S: $-151.7, -153.3^\circ$) while for **4** the conformation changes to *gauche*, *gauche* (*sc*, *sc*; dihedral \angle C–S–Sn–S: $51.9, 51.9^\circ$). The significance of this is the alignment of sulfur lone pairs along the C–S–Sn–S–C moiety, which we have explained more fully elsewhere as it is a general phenomenon. 35

Compound **5** (Fig. 4) also adopts a *cis*, *cis* arrangement of thiolate and dithiocarbamate groups, though detailed analysis of the structure is somewhat clouded by the disorder in the phenyl group based upon C(17). In general, however, the electron-withdrawing C_6H_5 group generates similar features to those seen in **6** *i.e.* weakening of the Sn–S(thiolate) [2.473(1), 2.480(1) Å], strengthening of Sn–S(dithiocarbamate) [2.546(1), 2.552(1) Å] and making chelation more symmetrical, at least for one ligand [2.573(1), 2.639(1) Å]. The inter-thiolate \angle S–Sn–S [88.85(4)°] is intermediate between the values for **4** and **6**, and the dihedral S–Sn–S–C angles are consistent with a distorted *trans*, *gauche* conformation [$-83.1, 154.8$ or -178.3°]. These findings are also in line with analysis presented above and elsewhere. 35

Thermal decomposition studies

In order to assess the potential of compounds **1**, **4**, **6** for the formation of tin sulfides, their thermal decompositions, along with that of the tin(II) species $(\text{Et}_2\text{NCS}_2)_2\text{Sn}$ (**7**), have been assessed by a combination of TGA and Mössbauer methods. For the Mössbauer experiments, the selected compound was

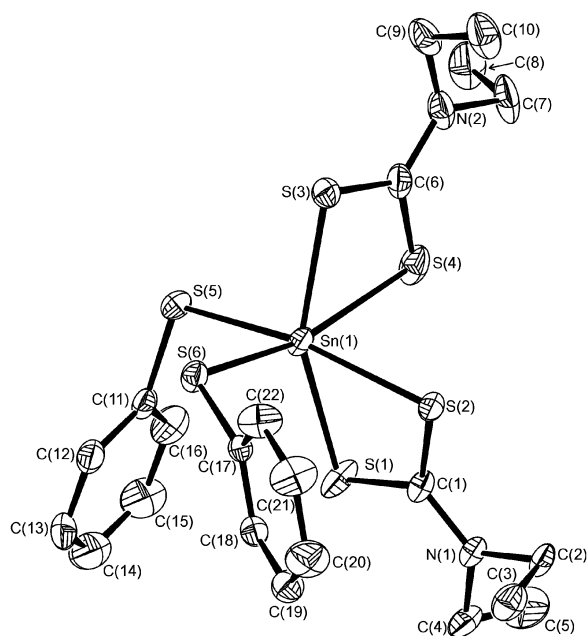


Fig. 4 The asymmetric unit of **5**; thermal ellipsoids are at the 30% probability. Sn(1)–S(1) 2.546(1), Sn(1)–S(2) 2.573(1), Sn(1)–S(3) 2.552(1), Sn(1)–S(4) 2.639(1), Sn(1)–S(5) 2.473(1), Sn(1)–S(6) 2.480(1) Å; S(1)–Sn(1)–S(2) 70.83(4), S(1)–Sn(1)–S(3) 156.30(5), S(1)–Sn(1)–S(4) 89.60(5), S(1)–Sn(1)–S(5) 97.11(4), S(1)–Sn(1)–S(6) 105.71(5), S(2)–Sn(1)–S(3) 96.36(4), S(2)–Sn(1)–S(4) 87.57(4), S(2)–Sn(1)–S(5) 167.94(4), S(2)–Sn(1)–S(6) 94.17(4), S(3)–Sn(1)–S(4) 69.51(5), S(3)–Sn(1)–S(5) 95.01(4), S(3)–Sn(1)–S(6) 94.80(4), S(4)–Sn(1)–S(5) 92.67(5), S(4)–Sn(1)–S(6) 164.32(5), S(5)–Sn(1)–S(6) 88.85(4)°.

placed into a dried Schlenk tube against a dry N_2 counterflow. The compound was then heated at 3° min^{-1} to the desired temperature under static N_2 , where it was held for two hours. The resulting Mössbauer spectra were compared with those of the starting materials and known spectra of SnS ($IS = 3.26$, $QS = 0.57 \text{ mm s}^{-1}$), SnS_2 ($IS = 0.87$, $QS = 0.00 \text{ mm s}^{-1}$) and Sn_2S_3 ($IS = 1.21, 3.31$; $QS = 0.00, 0.70 \text{ mm s}^{-1}$, for the two tin sites, respectively).⁴⁶ Additional XRD and Raman analyses have also been carried out to identify the nature of the decomposition product(s). The latter show diagnostic spectra for each of the three common tin sulfides: SnS_2 317, 209 cm^{-1} ; Sn_2S_3 307, 251, 234, 183, 71, 60, 52 cm^{-1} ; SnS 288, 220, 189, 163, 96 cm^{-1} .¹⁸

Following this procedure, $(\text{Et}_2\text{NCS}_2)_4\text{Sn}$ (**1**) decomposed at 200 °C to leave a species with $IS = 0.97$, $QS = 0.66 \text{ mm s}^{-1}$, which we assign to **3**, rather than SnS_2 , on the basis of a clearly resolvable quadrupole splitting (Fig. 5a). At 375 °C under N_2 , SnS_2 is formed and this has been confirmed by XRD and Raman spectroscopy. XRD reveals that the sample is primarily berndtite (*ca.* 90%) mixed with traces of SnS_2 -4H polytype; SnS (herzenbergite) is also present at *ca.* 10% level. The measured crystallographic data [hexagonal, $a = 3.64(1)$; $c = 5.89(1)$ Å] compare well with literature values for SnS_2 ($a = 3.62$ – 3.65 , $c = 5.85$ – 5.90 Å); crystallite size from line broadening was estimated as 350 Å. The deposition of SnS_2 is also confirmed by Raman bands at 316 and 210 cm^{-1} . The sample does however contain residual organic matter (C 5.45, H 0.36, N 0.95%).

In contrast, decomposition at 600 °C leads to the formation of nanocrystalline SnO_2 (XRD: cassiterite) with no evidence for the formation of tin sulfides. The residual organic content of the sample is low (C 1.12, H 0.34, N 0.00%).

For comparison, we have carried out TGA analysis of our samples at atmospheric pressure under a N_2 flow. The TGA of **1** (Fig. 5c) shows the formation of **3** by 250 °C (observed mass loss: 33.0; theoretical 34.3%); between 250 and 375 °C further decomposition leads to SnS_2 (observed residual mass: 33.0; theoretical 31.9%) and finally a species with mass corresponding to either SnS or SnO_2 by 650 °C (observed residual mass: 25.6; theoretical 25.9%). These findings are consistent with the

decomposition of bulk samples under static N_2 described above. However, the inflection point at *ca.* 300 °C corresponding to the formation of **7** by loss of $[\text{Et}_2\text{NC}(\text{S})\text{SS}(\text{S})\text{CNET}_2]$ (40% weight loss) suggests a more complex picture in which two decomposition mechanisms may be competing, as there is no TGA evidence that **3** itself eliminates sulfur to form **7** (see below, Fig. 5b).

There are conflicting reports in the literature as to the mechanism of decomposition of **1**. Bratspies³³ has claimed by TGA that **1** decomposes initially to give $(\text{Et}_2\text{NCS}_2)_2\text{Sn}$ (**7**) along with tetraethylthiuram disulfide $[\text{Et}_2\text{NC}(\text{S})\text{SS}(\text{S})\text{CNET}_2]$. Perry⁴⁷ has claimed that **7** decomposes in dry N_2 to give tin metal, and thus in air would provide a mechanism for the formation of SnO_2 , which we have also noted is present as a minor component in the Mössbauer spectra of samples of **1** heated to *ca.* 300 °C and is the final decomposition product of a bulk sample heated to 600 °C. However, Bratspies has repeated the TGA of pure **7** at $T < 600 \text{ K}$ and has claimed the formation of SnS , CS_2 and $(\text{Et}_2\text{N})_2\text{C}=\text{S}$.⁴⁸ To complicate matters, Bratspies has also claimed that tetraethylthiuram disulfide formed in the decomposition of **1** undergoes sulfur elimination to form the monosulfide $[\text{Et}_2\text{NC}(\text{S})\text{S}(\text{S})\text{CNET}_2]$ and that the extruded sulfur oxidises **7** to $[(\text{Et}_2\text{NCS}_2)_2\text{SnS}]_2$ *in situ*, which then further decomposes through a series of unidentified intermediates to leave SnS by 400 °C.³³ In our hands, however, the TGA of commercially

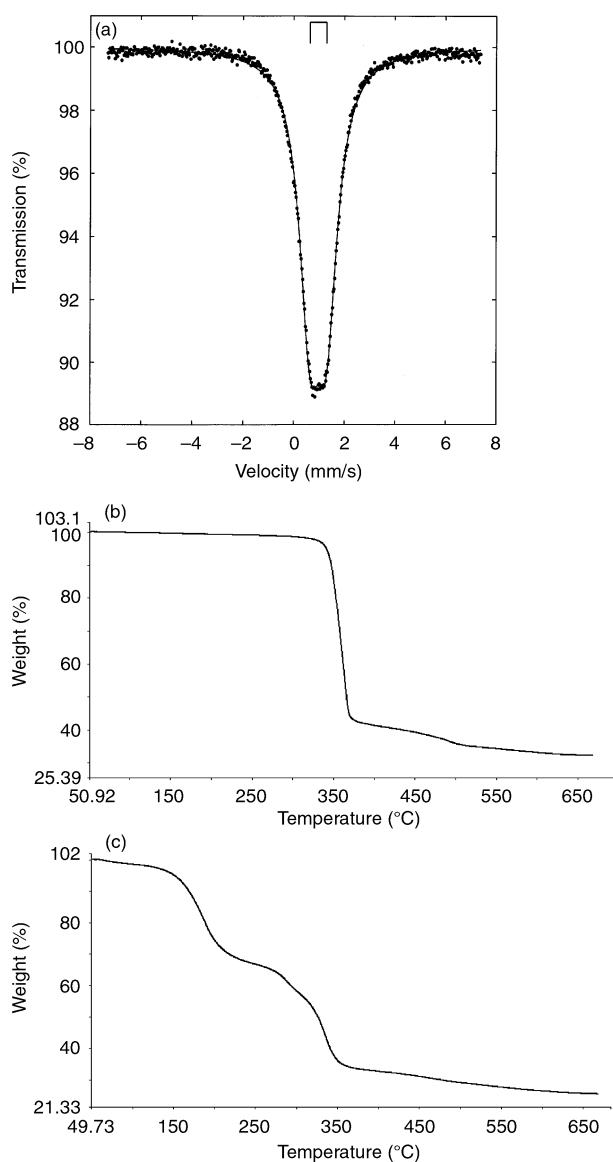


Fig. 5 (a) Mössbauer spectrum of the product obtained by heating **1** at 200 °C and identified as **3**, (b, c) the TGA of **3** and **1**, respectively.

available tetraethylthiuram disulfide shows it loses almost all its mass (*ca.* 95%) in a single step between 250 and 325 °C with no evidence for the stepwise elimination of sulfur. SnS₂ and SnO₂ have both been identified as products of the decomposition of [(*n*-ClC₆H₄)₂NCS₂]₂Sn (*n* = 2, 3, 4) in static air.^{49,50} It should be noted, however, that in all of the above SnS and SnO₂ are indistinguishable in simple mass terms

To rationalise the above findings we propose the following: the decomposition of **1** appears to go by the sequential elimination of two equivalents tetraethylthiuram disulfide. After one equivalent is lost, the Sn(dtc)₂ remaining will readily react with/abstract sulfur from tetraethylthiuram disulfide to form **3**, provided the temperature is below *ca.* 325 °C at which point the volatility of the disulfide causes its separation from the tin-containing residue. In contrast, decomposition at 600 °C seems to promote the elimination of two equivalents of tetraethylthiuram disulfide and its removal from the residue before sulfur abstraction takes place; the remaining tin metal combines with oxygen from either the glass surface or the N₂ used to backfill the Schlenk to generate SnO₂. In this latter respect, the decomposition of **1** follows that which we have previously described for homoleptic thiolates (RS)₄Sn, which also deposit tin oxide films in the absence of a secondary sulfur source.²¹

The sulfide-bridged dimer [(Et₂NCS₂)₂SnS]₂ (**3**) appears to be a key intermediate in the thermal decomposition chemistry of (Et₂NCS₂)₄Sn. The facile formation of this species from **1** in solution is not, however, consistent with **7** as an intermediate, and its formation by a concerted mechanism (see above) seems more likely in solution.

The TGA of **3** (Fig. 5b) shows clean decomposition between 325 and 375 °C, which formally corresponds to the elimination of [Et₂NC(S)]₂S and leaves SnS₂ (observed residual mass: 42.0; theoretical: 40.9%; Raman: 317, 210 cm⁻¹); further heating to 500 °C affords SnS as prismatic plates (observed residual mass: 34.0; theoretical 33.7%; Raman: 288, 218, 182, 161, 94 cm⁻¹) along with traces of Sn₂S₃ (Raman: 307 cm⁻¹).

Both (Et₂NCS₂)₂(RS)₂Sn [R = Cy (**4**), CF₃CH₂ (**6**)] behave similarly. The EI (70 eV) mass spectra of both compounds contain no tin-containing fragments but instead are dominated by species such as RSSR, RSS/RSSH and RSH. There is no evidence for fragments based on [Et₂NCS₂]₂ *e.g.* tetraethylthiuram disulfide. It appears that both compounds decompose *via* a common intermediate, namely (Et₂NCS₂)₂Sn (**7**), *via* loss or RSSR. The behaviour thus parallels the homoleptic thiolates (RS)₄Sn, which we have found in CVD experiments consistently give films of Sn₃O₄ unless H₂S is present, in which case tin sulfides are deposited (the nature of the sulfide being temperature dependent).²¹ It appears that (PhS)₄Sn decomposes *via* loss of PhSSPh to give first (PhS)₂Sn and subsequently tin metal, which then gets oxidised to either an oxide or a sulfide depending on conditions. We have found that heating (CyS)₂Sn in refluxing toluene produces a tin mirror on the walls of the reaction vessel, while the EI mass spectrum (70 eV) of this compound contains no tin-containing ions but is dominated by the fragments CySSCy, CySSH and Cy.

The Mössbauer spectrum of the products of the decomposition of **4** at 200 °C confirms the formation of **7** (IS = 3.23, QS = 1.78 mm s⁻¹) though the line width (1.03 mm s⁻¹) is broader than in pure **7** (0.81 mm s⁻¹). Microanalysis of the unpurified residue is also consistent with the formation of **7** [Found(calc. for C₁₀H₂₀N₂S₄Sn): C 29.9(28.9), H 5.17(4.87), N 4.81(6.75)%]. TGA of both **4** and **6** are broadly similar and both decompose in essentially two stages. For **6**, there is *ca.* 44% mass loss between 120 and 250 °C which correlates with the loss of [Et₂NCS₂]₂ (theoretical mass loss: 46%), in excess of that expected for loss of CF₃CH₂SSCH₂CF₃ (calculated mass decrease: 35.7%) and inconsistent with the decomposition of a bulk sample at 200 °C (above). However, a further loss of 41% mass between 250 and 325 °C is consistent with the elimination of [Et₂NC(S)]₂S [or its decomposition products, CS₂ and

(Et₂N)₂C=S] from the intermediate **7** (calculated mass decrease: 41.0%). The final residual mass (15.5%) is lower than that calculated for SnS (23.4%) and is probably a result of evaporation of the volatile **6** in the early stages of the experiment, which is the explanation for a mass loss greater than that expected for elimination of RSSR during the initial formation of intermediate **7**. In other work we have noted that (CF₃CH₂S)₄Sn is a highly volatile liquid with a boiling point of 35 °C, indicating the effect on volatility of the fluoroalkyl groups.⁵¹ The Mössbauer study of the decomposition of **4** (above) also rules out (RS)₂Sn as a primary decomposition intermediate.

The TGA of **4** similarly shows initial decomposition between 145 and 250 °C (*ca.* 55%) with a second process operating at 270–325 °C resulting in a further 21% weight loss. The mass remaining at this stage (24.4%) is in good agreement with the final product being SnS (theoretical 23.4%), though further weight loss accrues up to 500 °C (20.5%), presumably by loss of sulfur.

Formation of SnS at *T* > 325 °C has been confirmed by decomposition of **4** under static N₂ at 400 °C. The XRD pattern correlates with that of the mineral herzenbergite (orthorhombic, *a* = 4.33, *b* = 11.20, *c* = 3.98 Å; lit.^{52–54} *a* = 4.30–4.33, *b* = 11.18–11.21, *c* = 3.98–4.02 Å); crystallite size from line broadening was estimated as 550 Å. The deposition of SnS is also confirmed by Raman bands at 289, 218, 182, 162 and 96 cm⁻¹. There is some organic matter still remaining (C 2.0, H 0.06, N 0.03%).

The two TGA processes are directly comparable as the relative masses of both **4** and **6** are essentially identical (645), as are the relative masses of the two differing thiolate ligands (115). The initial weight loss in the case of **4** (*ca.* 55%) is greater than expected for loss of CySSCy alone, which, given the lower volatility of **4** compared to **6**, suggests that a second decomposition process is operative. The crystallography here can be constructive, as we have noted the effect of the CF₃CH₂S ligand is such that the Sn–S(thiolate) bond is weakened at the expense of stronger dithiocarbamate chelation. In addition, the conformational preference for the (CF₃CH₂S)₂Sn moiety leads to a narrower <S–Sn–S and closer S ⋯ S approach. We have shown elsewhere³⁵ that MOs associated with the lone pairs on sulfur can encourage S–S bond formation and this would appear particularly facile in the case of **6**. For **4**, on the other hand, the Sn–S(thiolate) bond is stronger, dithiocarbamate chelation weaker, the <S–Sn–S involving thiolate groups wider and hence S ⋯ S longer, all of which conspire to make elimination of CySSCy less facile while elimination of [Et₂NCS₂]₂ is promoted. We thus suggest that in the case of **4**, elimination of CySSCy remains the dominant first step in the decomposition, but that some elimination of [Et₂NCS₂]₂ is also possible. The broadened lines in the Mössbauer spectrum of the decomposition product of **4** (see above) are also consistent with the presence of a second species; Mössbauer data for pure (CyS)₂Sn are IS = 3.04, QS = 1.74, FWHH = 0.85 mm s⁻¹.⁵⁵

The complexity of the thermal decomposition of **4** is also manifest in experiments designed to assess the CVD potential of this precursor. Initially, the precursor **4** was held under a static N₂ atmosphere and heated to 200 °C in a tube furnace, while external to the furnace was placed a glass slide, independently heated by a ceramic infrared heater to a temperature of 550 °C; any volatile material produced from heating **4** would be expected to decompose and deposit on the slide. Under these conditions, a yellow film is deposited which Raman analysis indicates is SnS₂ (315 cm⁻¹). In contrast, when **4** is heated to 400 °C under N₂ (glass substrate still at 550 °C) the film consists of a leading edge of yellow material analysed as SnS₂ (Raman: 311–314 cm⁻¹ over a variety of locations), followed by a large area of grey/black film which is mainly SnS (Raman: 221, 185, 159, 95 cm⁻¹) with traces of Sn₂S₃ incorporated (Raman: 306 cm⁻¹).

The quality of SnS₂ films can be enhanced by repeating the experiments at low pressure and with the precursor heated to 350 °C. The hard, transparent coating thus deposited shows a refringence pattern due to a film of significant thickness and again analyses as SnS₂ (Raman: 315 cm⁻¹). Our previous attempts to deposit SnS₂ from either single- or dual-source precursors have always generated soft, powdery films typical of formation in the gas phase and subsequent diffusion to the substrate surface. In contrast, the SnS₂ deposited from **4** under LPCVD conditions is more typical of a surface-controlled reaction, which is possibly bi-molecular as the outcome is different to the decomposition of **4** under static conditions.

Conclusions

Decomposition of (Et₂NCS₂)₄Sn to SnS₂ takes place *via* [(Et₂NCS₂)₂SnS]₂, with each pair of dithiocarbamate ligands effectively losing [Et₂NC(S)]₂S; however, at least in the solid state, this occurs by initial elimination of tetraethylthiuram disulfide from which sulfur is abstracted as long as the tin and disulfide remain in contact. At higher temperatures complete removal of two equivalents of tetraethylthiuram disulfide leads to *in situ* formation of Sn(o) and ultimately SnO₂ is generated.

Mixed-ligand species (Et₂NCS₂)₂(RS)₂Sn can be synthesised *inter alia* by a ligand redistribution between (RS)₄Sn and (Et₂NCS₂)₄Sn. These heteroleptic species decompose to SnS by initial elimination of RSSR to afford (Et₂NCS₂)₂Sn and subsequent loss of [Et₂NC(S)]₂S. The two families of compound, (R₂NCS₂)₄Sn and (RS)₂(Et₂NCS₂)₂Sn, thus provide single-source materials for bulk SnS₂ and SnS, respectively, by virtue of their differing decomposition pathways. The formation of SnS directly from (Et₂NCS₂)₂(RS)₂Sn at temperatures as low as 350 °C is in contrast to other deposition routes in which tin(II) sulfide is formed by thermal decomposition of SnS₂ at *T* > ca. 500 °C *i.e.* thermal control of film composition.

From the CVD perspective, (Et₂NCS₂)₂(CF₃CH₂S)₂Sn appears sufficiently volatile to merit further study. However, preliminary experiments with the less-volatile (Et₂NCS₂)₂(CyS)₂Sn show that films can be grown, particularly at low pressure, but that a different growth mechanism is operative to that observed in the bulk *i.e.* SnS₂, rather than SnS, is the primary deposition product. CVD experiments using the dimer [(Et₂NCS₂)₂SnS]₂ are also in progress.

Experimental

Infrared spectra were recorded as hexachlorobutadiene mulls between KBr plates using a Nicolet 510P FT-IR spectrophotometer, and elemental analyses were performed using a Carlo-Erba Strumentazione E.A. model 1106 microanalyser operating at 500 °C. ¹H and ¹³C NMR spectra were recorded on a Jeol JNM-GX270 FT spectrometer and ¹¹⁹Sn NMR spectra were recorded on a Jeol JNM-EX400 FT machine, all using saturated CDCl₃ solutions unless indicated otherwise. Details of our Mössbauer spectrometer and related procedures are given elsewhere.⁵⁶ Thermogravimetric studies were performed on a Perkin Elmer TGA7 analyser. Dry solvents were obtained by distillation under an inert atmosphere from the following drying agents: sodium–benzophenone (toluene, ether, THF), calcium hydride (CH₂Cl₂), sodium (hexane). Standard Schlenk techniques were used throughout. Starting materials were commercially obtained and used without further purification.

Syntheses

(Et₂NCS₂)₄Sn (**1**). This was prepared by a known route and exhibited spectroscopic properties identical to those reported.²⁵ ¹¹⁹Sn NMR: –766 (100%); –765 (30%), 768 (32%) ppm.

[Buⁿ(Me)NCS₂]₄Sn (**2**). **2** was prepared from [Buⁿ(Me)NC-S₂Li (**8**) and SnCl₄. Compound **8** was prepared by a modification of the method of O'Brien *et al.*⁵⁷ involving the addition of BuⁿLi in hexane (20.3 ml 2.5 M, 51.0 mmol) to *N*-methyl *N*-butylamine (6.0 ml, 50.7 mmol) in cold hexane (50 ml). After stirring for 30 mins at room temperature redistilled CS₂ (3.1 ml, 51.5 mmol) was added dropwise, causing an exothermic reaction and formation of a yellow precipitate. After stirring for several hours, the supernatant was removed by cannula filtration and the residual solid (**8**) washed with hexane (40 ml) before drying *in vacuo* (yield 7.76 g, 90%).

SnCl₄ (0.4 ml, 3.42 mmol) was added dropwise to a suspension of **8** (2.33 g, 13.7 mmol) in CH₂Cl₂ (40 ml) yielding a white precipitate of LiCl in an orange solution. After stirring overnight at room temperature, the precipitate was separated by filtration and the filtrate concentrated *in vacuo* to a viscous orange oil. Trituration of this oil with pentane (4 × 20 ml) afforded **2** as a yellow/orange solid (1.69 g, 64%), mp 88 °C. Found (calc. for C₂₄H₄₈N₄S₈Sn): C, 37.7(37.5), H, 6.33(6.30), N, 7.22(7.30)%. ¹H NMR: δ 0.97 (t, 3H, CH₂CH₃), 1.38 (m, 2H, CH₂), 1.77 (m, 2H, CH₂), 3.37 (s, 3H, NCH₃), 3.67 (t, 2H, CH₂N; *J* = 7.8 Hz). ¹³C NMR: δ 196.0 (CN), 60.5 (NCH₂), 44.8 (NCH₃), 29.2 (CH₂), 20.3 (CH₂), 14.1 (CH₃) ppm. ¹¹⁹Sn NMR: –786 ppm. Mössbauer: IS = 0.70, QS = 0.00, Γ = 0.68 mm s⁻¹.

[(Et₂NCS₂)₂SnS]₂ (**3**). Sn(S₂CNEt₂)₄ (1.50 g, 1.99 mmol) was dissolved in dichloromethane (50 ml). The solution was refluxed under nitrogen for 24 h, causing a colour change from red–orange to yellow and the formation of a small amount of white precipitate. Further reflux (24 h), subsequent filtration and slow evaporation of the solvent in air yielded colourless crystals of **3** (0.50 g, 33%), mp 272 °C. Found (calc. for C₂₂H₄₀S₁₀N₄Sn₂): C, 27.0(26.8), H, 4.56(4.47), N, 6.22(6.26)%. ¹H NMR: δ 1.49 (t, 3 H, CH₃; *J* = 7.3 Hz), 3.04 (q, 2H, CH₂; *J* = 7.3 Hz). ¹³C NMR: δ 11.4 (CH₃), 50.4 (CH₂) ppm. ¹¹⁹Sn NMR (CDCl₃): –736 ppm. Mössbauer: IS = 0.96, QS = 0.55, Γ = 0.92 mm s⁻¹.

(Et₂NCS₂)₂(C₆H₁₁S)₂Sn (**4**). Sn(S₂CNEt₂)₄ (992 mg, 1.39 mmol) and Sn(SC₆H₁₁)₄ (808 mg, 1.39 mmol) were dissolved in toluene (total volume 100 ml). The solution was stirred at room temperature for 8 h, causing a colour change from orange to yellow. After this time the solution was concentrated by removal of ca. 80% of the solvent *in vacuo*. Standing at –30 °C overnight gave bright yellow crystals of **4**, (1.20 g, 67%), which were isolated by filtration. mp 114–114.5 °C. Found (calc. for C₂₂H₄₂S₆N₂Sn): C, 41.4(40.9), H, 6.59(6.56), N, 4.34(4.34)%. ¹H NMR (C₆D₆): δ 0.75 (t, 6 H, CH₃; *J* = 7.1 Hz), 1.47 (d, 4 H, CH₂; *J* = 10.8 Hz), 1.80 (d, 4 H, CH₂; *J* = 10.7 Hz), 2.47 (d, 2 H, CH₂; *J* = 9.6 Hz), 3.07 (q, 4 H, NCH₂; *J* = 7.0 Hz), 3.83 (m, 1 H, CH). ¹³C NMR (C₆D₆): δ 198.8 (CS₂), 50.9 (NCH₂), 44.5, 38.9, 27.2, 26.1 (C₆H₁₁), 11.7 (CH₃) ppm. ¹¹⁹Sn NMR (C₆D₆): –649 ppm. Mössbauer: IS = 1.05, QS = 0.55, Γ = 0.81 mm s⁻¹.

(Et₂NCS₂)₂(C₆H₅S)₂Sn (**5**). *Method 1*. Using the methodology described above for **4**, **5** was prepared from (PhS)₄Sn (490 mg, 0.88 mmol) and **1** (663 mg, 0.88 mmol) in toluene (100 ml) for 2 h under reflux. Recrystallisation from diethyl ether (20 ml) gave yellow crystals of **5** (367 mg, 56%).

Method 2. [Ph₄P⁺][[(PhS)₃Sn]⁻]⁵⁸ (1.00 g, 1.27 mmol) was dissolved in CH₃CN (50 ml) and an excess of tetraethylthiuram disulfide (0.50 g, 1.69 mmol) added. After stirring for 2 h, the solvent was evaporated *in vacuo* and the residue recrystallised from the minimum quantity of CH₃CN.

Method 3. (PhS)₄Sn (0.24 g, 0.43 mmol) was dissolved in toluene (50 ml) and Cu(S₂CNEt₂)₂ (0.16 g, 0.43 mmol) added. The resulting solution was refluxed for 2 h at 60 °C, causing a colour change from black–brown to yellow–brown. The solution was then stirred at RT overnight. The solvent was removed *in vacuo* and the residue dissolved in CHCl₃. Addition

Table 1 Crystal data and structure refinement for **3**, **4**, **5** and **6**

	3	4	5	6
Empirical formula	C ₂₂ H ₄₂ Cl ₆ N ₄ S ₁₀ Sn ₂	C ₂₂ H ₄₂ N ₂ S ₆ Sn	C ₂₂ H ₃₀ N ₂ S ₆ Sn	C ₁₄ H ₂₄ F ₆ N ₂ S ₆ Sn
<i>M</i>	566.64	645.63	633.53	645.40
<i>T</i> /K	170(2)	293(2)	170(2)	170(2)
Crystal system	Monoclinic	Monoclinic	Monoclinic	Monoclinic
Space group	<i>P</i> 2 ₁ / <i>a</i>	<i>C</i> 2/ <i>c</i>	<i>Aa</i>	<i>P</i> 2 ₁ / <i>n</i>
<i>a</i> /Å	10.0970(1)	18.476(2)	11.8630(3)	15.891(1)
<i>b</i> /Å	22.1450(2)	9.453(1)	14.8960(5)	9.899(1)
<i>c</i> /Å	10.3630(1)	17.530(2)	15.7620(5)	16.623(1)
β /°	108.450(1)	101.38(1)	93.094(2)	102.42(1)
<i>V</i> /Å ³	2198.05(4)	3001.5(6)	2781.3(2)	2553.7(1)
<i>Z</i>	2	4	4	4
μ (Mo-K α)/mm ⁻¹	1.999	1.282	1.383	1.539
Independent reflections	6408 [<i>R</i> (int) = 0.0381]	2348 [<i>R</i> (int) = 0.0115]	5621 [<i>R</i> (int) = 0.0571]	5860 [<i>R</i> (int) = 0.0382]
Final <i>R</i> indices [<i>I</i> > 2 σ (<i>I</i>)]	<i>R</i> ₁ = 0.0243 <i>wR</i> ₂ = 0.0573	<i>R</i> ₁ = 0.0415 <i>wR</i> ₂ = 0.1016	<i>R</i> ₁ = 0.0355 <i>wR</i> ₂ = 0.0959	<i>R</i> ₁ = 0.0340 <i>wR</i> ₂ = 0.1189
<i>R</i> indices (all data)	<i>R</i> ₁ = 0.0275 <i>wR</i> ₂ = 0.0587	<i>R</i> ₁ = 0.0595 <i>wR</i> ₂ = 0.1056	<i>R</i> ₁ = 0.0383 <i>wR</i> ₂ = 0.0999	<i>R</i> ₁ = 0.0422 <i>wR</i> ₂ = 0.1273

of cold pentane and immediate filtration yielded a yellow orange solid (0.07 g, 29%). mp 113 °C. Found(calc. for C₂₂H₃₀S₆N₂Sn): C, 41.8(41.7), H, 4.79(4.77), N, 4.54(4.42)%. ¹H NMR: δ 0.38 (t, 3 H, CH₃; *J* = 7.1 Hz), 2.65 (q, 2H, CH₂; *J* = 7.1 Hz), 6.83 (m, 3H, C₆H₅), 7.69 (d, 2H, C₆H₅; *J* = 7.2 Hz). ¹³C NMR: δ 198.7 (CS₂), 51.3 (CH₂), 188.8, 137.6, 127.2 (C₆H₅), 51.3 (CH₂), 12.0 (CH₃) ppm. ¹¹⁹Sn NMR: -666 ppm. Mössbauer: IS = 1.01, QS = 0, Γ = 1.14 mm s⁻¹.

(Et₂NCS₂)₂(CF₃CH₂S)₂Sn (**6**). To a yellow solution of (C₅H₅)₂Sn⁵⁹ (561 mg, 2.24 mmol) in Et₂O (20 ml) CF₃CH₂SH (0.4 ml, 4.50 mmol) was added dropwise forming a deep orange solution. After stirring at room temperature for 1 h, tetraethylthiuram disulfide (667 mg, 2.25 mmol) was added and the solution was heated to reflux for ca. 5 min, during which time the solution turned a paler yellow/orange. After stirring at room temperature for 1 h, the solvent was removed *in vacuo* leaving (CF₃CH₂S)₂Sn(S₂CNEt₂)₂ as an orange solid. Recrystallisation from THF (5 ml) at -30 °C gave pale orange crystals (1.18 g, 82%). ¹H NMR: 1.28 (t, 6H, CH₃, ³*J*_{H-H} = 7.1 Hz), 3.49 (q, 2H, CH₂CF₃, ³*J*_{H-F} = 10.1 Hz), 3.67 (q, 4H, CH₂CH₃, ³*J*_{H-H} = 7.1 Hz); ¹³C NMR: 11.9 (s, CH₃), 32.3 (q, CH₂CF₃, ²*J*_{C-F} = 33 Hz), 51.6 (s, CH₂CH₃), 126.3 (q, CF₃, ¹*J*_{C-F} = 275 Hz), 196.4 (s, quarternary C); ¹⁹F NMR: -66.9 (t, ³*J*_{F-H} = 9.8 Hz); ¹¹⁹Sn NMR: -661.

(Et₂NCS₂)₂Sn (**7**). SnCl₂·2H₂O (4.00 g, 17.8 mmol) and [Et₂NCS₂]₂Na·3H₂O (8.02 g, 35.5 mmol) were dissolved in deoxygenated H₂O (100 ml) with the immediate formation of a yellow precipitate of **6**. After 30 mins stirring at room temperature the precipitate was isolated by filtration and dried *in vacuo* giving Sn(S₂CNEt₂)₂ as a yellow solid (6.71 g, 91%). Spectroscopic properties were identical to those reported.²⁸

Crystallography

Crystallographic data for compounds **3**, **4**, **5** and **6** are summarised in Table 1. Data for **4** were collected on a CAD4 automatic 4-circle diffractometer, while those for **2**, **3** and **5** were implemented on a Nonius KappaCCD diffractometer. The asymmetric unit in both **3** and **4** consisted of one half of a molecule, the remaining portions being generated respectively by either an inversion centre or a 2-fold rotation axis implicit in the respective space groups. Full matrix anisotropic refinement was implemented in the final least-squares cycles throughout. All data were corrected for Lorentz and polarisation and, with the exceptions of **4** and **5**, for extinction. An absorption correction (multiscan) was applied to data for **3**, **5** and **6** (maximum and minimum transmission factors for **3**, **5**, and **6**: 1.036, 0.935; 1.025, 0.969 and 1.061, 0.967 respectively). Hydrogens were included at calculated positions throughout. The phenyl ring containing carbons C17–C22 in **5** was disordered in a 1 : 1 ratio with positions C17'–C22'. Both parts were refined anisotropic-

ally as rigid hexagons. Structure determination and refinement was achieved using the SHELX suite of programs;^{60,61} drawings were produced using ORTEP.⁶²

CCDC reference numbers 157255–157258.

See <http://www.rsc.org/suppdata/dt/b1/b108509n/> for crystallographic data in CIF or other electronic format.

Acknowledgements

We thank the EPSRC and Pilkington plc for support and JREI/EPSRC for the purchase of the diffractometer.

References

- T. Jiang and G. A. Ozin, *J. Mater. Chem.*, 1998, **8**, 1099.
- G. Valiukonis, D. A. Guseinova, G. Krivaite and A. Sileica, *Phys. Status Solidi B*, 1986, **135**, 299.
- G. Valiukonis, D. G. Krivaile and A. Sileica, *Phys. Status Solidi B*, 1990, **135**, 229.
- M. T. S. Nair and P. K. Nair, *J. Phys. D: Appl. Phys.*, 1991, **24**, 75.
- J. A. Woolam and R. B. Soloano, *Mater. Sci. Eng.*, 1977, **31**, 289.
- D. O'Hare, W. Jaegermann, D. L. Williams, F. S. Ohuchi and B. A. Parkinson, *Inorg. Chem.*, 1988, **27**, 537.
- D. O'Hare, C. Formstone, J. Hodby, M. Kemoo, E. Fitzgerald and P. A. Cox, *J. Chem. Soc., Chem. Commun.*, 1990, 11.
- S. Lopez and A. Ortiz, *Semicond. Sci. Technol.*, 1994, **9**, 2130.
- T. Chaddopadhyay, J. Pannetier and H. G. v. Schnering, *J. Phys. Chem. Solids*, 1986, **44**, 879.
- M. T. S. Nair and P. K. Nair, *Semicond. Sci. Technol.*, 1991, **6**, 132.
- R. Engelken, H. McCloud, M. Slayton and E. Smith, *J. Electrochem. Soc.*, 1975, **134**.
- R. D. Engleken, H. E. McCloud, C. Lee, M. Slayton and H. Goreishi, *J. Electrochem. Soc.*, 1987, **134**, 2696.
- P. Boudjouk, D. J. Seidler, S. R. Bahr and G. J. McCarthey, *Chem. Mater.*, 1994, **6**, 2108.
- P. Boudjouk, D. J. Seidler, D. Grier and G. J. McCarthey, *Chem. Mater.*, 1996, **8**, 1189.
- H. M. Manasevit and W. I. Simpson, *J. Electrochem. Soc.*, 1975, **122**, 444.
- A. Ortiz, J. C. Alonso, M. Garcia and J. Toriz, *J. Semicond. Sci. Technol.*, 1996, **11**, 243.
- L. S. Price, I. P. Parkin, T. G. Hibbert and K. C. Molloy, *Adv. Mater.*, 1998, **4**, 222.
- L. S. Price, I. P. Parkin, A. M. E. Hardy, R. J. H. Clark, T. G. Hibbert and K. C. Molloy, *Chem. Mater.*, 1999, **11**, 1792.
- I. P. Parkin, L. S. Price, A. M. E. Hardy, R. J. H. Clark, T. G. Hibbert and K. C. Molloy, *J. Phys. IV*, 1999, **9**, Pr8.
- L. S. Price, I. P. Parkin, M. N. Field, A. M. E. Hardy, R. J. H. Clark, T. G. Hibbert and K. C. Molloy, *J. Mater. Chem.*, 2000, **10**, 527.
- G. Barone, T. G. Hibbert, M. F. Mahon, K. C. Molloy, L. S. Price, I. P. Parkin, A. M. E. Hardy and M. N. Field, *J. Mater. Chem.*, 2000, **11**, 464.
- I. P. Parkin, L. S. Price, T. G. Hibbert and K. C. Molloy, *J. Mater. Chem.*, 2001, **11**, 1486.
- M. B. Bochmann, *Chem. Vap. Deposition*, 1996, **2**, 85.
- P. O'Brien, J. R. Walsh, I. M. Watson, M. Motevalli and L. Henriksen, *J. Chem. Soc., Dalton Trans.*, 1996, 2491.

- 25 C. S. Harreld and E. O. Schlemper, *Acta Crystallogr., Sect. B*, 1971, **27**, 1964.
- 26 J. Potenza, R. J. Johnson and D. Mastropaolo, *Acta Crystallogr., Sect. B*, 1976, **32**, 941.
- 27 J. Potenza and D. Mastropaolo, *Acta Crystallogr., Sect. B*, 1973, **29**, 1830.
- 28 B. F. Hoskins, R. L. Martin and N. M. Rohde, *Aust. J. Chem.*, 1976, **29**, 213.
- 29 H. O. Davies, A. C. Jones, T. J. Leedham, M. J. Crosbie, P. J. Wright, N. M. Boag and J. R. Thompson, *Chem. Vap. Deposition*, 2000, **6**, 71.
- 30 R. Selvaraju, K. Panchanatheswaran and K. Venkatasubramanian, *Polyhedron*, 1994, **13**, 903.
- 31 Y. Zhou and D. S. Richeson, *J. Am. Chem. Soc.*, 1996, **118**, 10850.
- 32 H. Puff, G. Bertram, B. Ebeling, M. Franken, R. Gattermeyer, R. Hundt, W. Schuh and R. Zimmer, *J. Organomet. Chem.*, 1989, **379**, 235.
- 33 G. K. Bratspies, J. F. Smith, J. O. Hill and R. J. Magee, *Thermochim. Acta*, 1977, **19**, 361.
- 34 A. C. Fabretti and C. Preti, *J. Crystallogr. Spectrosc. Res.*, 1989, **19**, 957.
- 35 T. G. Hibbert, M. F. Mahon, K. C. Molloy, I. P. Parkin, L. S. Price and I. Silaghi-Dumitrescu, *J. Chem. Soc., Dalton Trans.*, 2001, 3435.
- 36 D. A. Fletcher, R. F. McMeeking and D. Parkin, *J. Chem. Inf. Comput. Sci.*, 1996, **36**, 746.
- 37 J. T. Huneke, K. Yamanouchi and J. H. Enemark, *Inorg. Chem.*, 1978, **17**, 3695.
- 38 R. A. Winograd, D. L. Lewis and S. J. Lippard, *Inorg. Chem.*, 1975, **14**, 2601.
- 39 A. L. Odom and C. C. Cummins, *Polyhedron*, 1998, **17**, 675.
- 40 K. Schulbert and R. Mattes, *Z. Naturforsch., Teil B*, 1994, **49**, 770.
- 41 D. L. Reger and J. E. Collins, *Inorg. Chem.*, 1995, **34**, 2473.
- 42 K. Brandt and W. S. Sheldrick, *J. Chem. Soc., Dalton Trans.*, 1996, 1237.
- 43 T. Kimura, N. Yasuoka, N. Kasai and M. Kakudo, *Bull. Chem. Soc. Jpn.*, 1972, **45**, 1649.
- 44 T. P. Lockhart, W. F. Manders, E. O. Schlemper and J. J. Zuckerman, *J. Am. Chem. Soc.*, 1986, **108**, 4074.
- 45 K. Kim, J. A. Ibers, O.-S. Jung and Y. S. Sohn, *Acta Crystallogr., Sect. C*, 1987, **43**, 2317.
- 46 A. Feltz, E. Schlenzig and D. Arnold, *Z. Anorg. Allg. Chem.*, 1974, **403**, 243.
- 47 D. Perry and R. A. Geanangel, *Inorg. Chim. Acta*, 1975, **13**, 185.
- 48 G. K. Bratspies, J. F. Smith, J. O. Hill and R. J. Magee, *Thermochim. Acta*, 1978, **27**, 307.
- 49 N. K. Kaushik, B. Bhushan and A. K. Sharma, *Thermochim. Acta*, 1984, **76**, 345.
- 50 N. K. Kaushik, G. R. Chattwal and A. K. Sharma, *Thermochim. Acta*, 1982, **58**, 231.
- 51 T. G. Hibbert, M. F. Mahon, K. C. Molloy, I. P. Parkin and L. S. Price, *J. Mater. Chem.*, 2001, **11**, 469.
- 52 W. E. Morganand and J. E. V. Wazer, *J. Chem. Phys.*, 1973, **77**, 96.
- 53 T. Shibata, Y. Mironushi, T. Miura and T. Kishi, *J. Mater. Sci.*, 1991, **26**, 5105.
- 54 C. A. Formstone, E. T. Fitzgerald, P. A. Cox and D. O'Hare, *Inorg. Chem.*, 1990, **29**, 3860.
- 55 T. G. Hibbert and K. C. Molloy, unpublished results.
- 56 K. C. Molloy, T. G. Purcell, K. Quill and I. Nowell, *J. Organomet. Chem.*, 1984, **267**, 237.
- 57 P. O'Brien, D. J. Otway and J. R. Walsh, *Thin Solid Films*, 1998, **315**, 57.
- 58 P. A. W. Dean, J. J. Vittal and N. C. Payne, *Can. J. Chem.*, 1985, **63**, 394.
- 59 E. O. Fischer and H. Grubert, *Z. Naturforsch., Teil B*, 1956, **11**, 423.
- 60 G. M. Sheldrick, SHELX 86S, A Computer Program for Crystal Structure Determination, University of Göttingen, Göttingen, 1986.
- 61 G. M. Sheldrick, SHELX 97L, A Computer Program for Crystal Structure Refinement, University of Göttingen, Göttingen, 1997.
- 62 P. McArdle, *J. Appl. Crystallogr.*, 1995, **28**, 65.